

PAPER • OPEN ACCESS

Theoretical Study of Unconventional Plasmons Formation within a Reduced-Size 1D Hubbard Model around a Quarter Filling

To cite this article: A. R. P. Tambunan *et al* 2019 *IOP Conf. Ser.: Mater. Sci. Eng.* **515** 012055

View the [article online](#) for updates and enhancements.

Theoretical Study of Unconventional Plasmons Formation within a Reduced-Size 1D Hubbard Model around a Quarter Filling

A. R. P. Tambunan, W. Wilwin, M. A. Majidi*

Department of Physics, Faculty of Mathematics and Natural Sciences, Universitas Indonesia, Kampus UI Depok, Depok 16424, Indonesia

*Corresponding author's email: aziz.majidi@sci.ui.ac.id

Abstract. Plasmons, which are conventionally known as quanta of electron plasma oscillations in a metal, were discovered unconventionally in an experiment of Strontium Niobate Oxide with oxygen enrichment ($\text{SrNbO}_{3.4}$). Plasmons that revealed in this experiment arose in the visible-ultraviolet range due to a confinement created by additional oxygens forming nanometer-spaced planes. This experimental background motivated us to study the formation of unconventional plasmons in the material by modeling a hypothetical system described by 5-sites linear chain Hubbard model around a quarter filling. The model was then solved by exact diagonalization (ED) method, from which we constructed the corresponding retarded Green function via Lehmann representation. Our interest was to calculate the optical response functions using Kubo formula of the linear response theory. Our results showed that the conventional plasmonic signals got modified by the presence of on-site Coulomb interactions. In addition, we observed that unconventional plasmons, behaving similarly to those found in the experiment, arose when the Coulomb intersite interaction was applied to the calculation.

Keywords: Unconventional plasmon, Hubbard model, quarter filling, $\text{SrNbO}_{3.4}$, ED method

1. Introduction

A journey of plasmonics researches in physics, especially in nanophotonics area was started from a phenomenon found on metallic films which showed energy losses as electrons passed through [1,2]. It was answered by Pines and Bohm by suggesting that the energy loss spectra originate from collective oscillations of electrons in metal at its plasma frequency [3,4]. This oscillation at plasma frequency is then referred to as plasmon [2]. Since then, various fascinating properties of plasmon are continuously being studied, such as its ability to localize light on metal surfaces and interfaces in sub-wavelength regions [5,6], and that all of them occur in a nanoscale region [7].

Recently, some pieces of researches on plasmonics are conducted in several ways moving forward to the discovery of plasmonics phenomena in non-metallic and insulating phase materials. There are several theoretical researches on plasmonics in topological insulators [6,8–10]. These studies show an interesting characteristic, namely their resonance frequencies, which are in the mid-infrared and terahertz spectral regions, can be tuned by varying the Fermi level or the wave vector [6,9]. A theoretical



study of 2D Hubbard model within extended DMFT reveals a possibility of plasmonics appearance in the insulating phase of strongly correlated systems [7].

In this study, we aimed to investigate the possibility of formation of plasmons in a reduced-size or confined one-dimensional non-metallic material. This study is motivated by an experimental report on Strontium Niobate Oxide with some oxygen enrichments ($\text{SrNbO}_{3+\delta}$) that show multiple unconventional plasmons generated by Nb-4d electrons confined within the nanometer-spaced extra oxygen planes [11]. This confinement leads to a good theoretical background to study such a system by using the reduced-size 1D model that incorporates electron-electron interaction in the calculations. The experimental study of Ref. [11] is supported by a semi-classical modeling (coupled oscillator model) to explain the experimental data. Although the results impressively mimic the experimental optical spectra, the underlying quantum mechanical process remains unclear since the model is merely semi-classical and phenomenological. To explore the underlying quantum mechanical mechanism in the more microscopic level, here, we present a theoretical study of Hubbard model on a reduced-size one-dimensional space around a quarter-filling. We hypothesize that the model would lead to a charge-ordered phase and reveal the optical spectra with the unconventional plasmonic behavior similar to those observed in the experimental data.

2. Model

We construct our model by considering a linear chain of atom with only as five atomic sites ($N = 5$) with equal spacing a between nearest-neighbors. Each atom is assumed to have only one atomic orbital of which on-site energy is taken to be the same for all atoms, which we set to be zero. Here, electrons can hop from one site to another with two possible spin states: up or down. The hopping integral is assumed non-zero only for the nearest-neighbor hopping with the hopping parameter denoted as $-t$. Electrons are considered to undergo Coulomb repulsion when two electrons of opposite spins happen to occupy the same atomic site, with the on-site interaction parameter U , and when they occupy different atoms within the nearest-neighbour with the inter-site interaction parameter V . With this picture in mind, we come up with our model that can be expressed in the second-quantised form as

$$H = -t \sum_{i,j,\sigma}^{i \neq j} c_{i\sigma}^\dagger c_{j\sigma} + U \sum_{i=1}^N n_{i\uparrow} n_{i\downarrow} + V \sum_{i=1}^{N-1} n_i n_{i+1}. \quad (1)$$

The first term of Equation 1 is the hopping term describing the energy needed for an electron to hop from one site to another. $c_{i\sigma}^\dagger$ and $c_{j\sigma}$ are the creation and annihilation operators, respectively, that create (annihilates) an electron at site i (j) with spin component σ . The second term is the on-site Coulomb repulsion where two electrons of opposite spins (subject to the Pauli exclusion principle) occupying the same atomic site feels an interaction strength U . While, the third term is the inter-site Coulomb repulsion where two electrons, regardless of their relative spin directions, occupying different atomic within nearest neighbor feel an interaction strength V [12,13]. Here $n_{i\sigma} = c_{i\sigma}^\dagger c_{i\sigma}$, with $n_i = \sum_{\sigma} n_{i\sigma}$, is the occupation number operator that counts the number of electrons occupying site i with spin component σ . If we expand all the summations in Equation 1, the hopping and the interaction terms read, respectively, as

$$\begin{aligned} H_{\text{hopping}} = -t & (c_{1\uparrow}^\dagger c_{2\uparrow} + c_{2\uparrow}^\dagger c_{1\uparrow} + c_{2\uparrow}^\dagger c_{3\uparrow} + c_{3\uparrow}^\dagger c_{2\uparrow} \\ & + c_{3\uparrow}^\dagger c_{4\uparrow} + c_{4\uparrow}^\dagger c_{3\uparrow} + c_{4\uparrow}^\dagger c_{5\uparrow} + c_{5\uparrow}^\dagger c_{4\uparrow} \\ & c_{1\downarrow}^\dagger c_{2\downarrow} + c_{2\downarrow}^\dagger c_{1\downarrow} + c_{2\downarrow}^\dagger c_{3\downarrow} + c_{3\downarrow}^\dagger c_{2\downarrow} \\ & + c_{3\downarrow}^\dagger c_{4\downarrow} + c_{4\downarrow}^\dagger c_{3\downarrow} + c_{4\downarrow}^\dagger c_{5\downarrow} + c_{5\downarrow}^\dagger c_{4\downarrow}) \end{aligned} \quad (2)$$

$$\begin{aligned} H_{\text{interaction}} = & U(n_{1\uparrow} n_{1\downarrow} + n_{2\uparrow} n_{2\downarrow} + n_{3\uparrow} n_{3\downarrow} + n_{4\uparrow} n_{4\downarrow} + n_{5\uparrow} n_{5\downarrow}) \\ & + V(n_1 n_2 + n_2 n_3 + n_3 n_4 + n_4 n_5). \end{aligned} \quad (3)$$

Note that Equation 1 is a modified version of the one-dimensional Hubbard model [14–16]. The standard one-dimensional Hubbard model itself usually applies for an extended system ($N \rightarrow \infty$) having translationally-invariant symmetry, with $V = 0$. Such a model is exactly solvable by means of the Bethe ansatz [15,16]. For our specific type of Hubbard model represented by the Hamiltonian in Equation 1, we shall use exact-diagonalization method [17] to solve it.

3. Methods

To solve the model using exact diagonalization method, we firstly need to define the basis set of independent states to form our Hilbert space. For a specific case of our interest, we consider a fixed number of electrons, i.e. $N_e = 3$, in our system. With this, there are $\frac{2N!}{N_e!(2N-N_e)!} = \frac{10!}{3!7!} = 120$ possible ways for the three electrons to arrange their states in the system. Here we have to tabulate all the basis kets $|\Phi_k^3\rangle$ ($k = 1, 2, \dots, 120$) corresponding to the 120 configurations before we use them for further steps of calculation. In Equation 4 below we display only a few first configurations as an example,

$$\begin{aligned} |\Phi_1^3\rangle &= c_{1\uparrow}^\dagger c_{2\uparrow}^\dagger c_{3\uparrow}^\dagger |0\rangle & |\Phi_2^3\rangle &= c_{1\uparrow}^\dagger c_{2\downarrow}^\dagger c_{3\downarrow}^\dagger |0\rangle & |\Phi_3^3\rangle &= c_{1\uparrow}^\dagger c_{2\uparrow}^\dagger c_{4\uparrow}^\dagger |0\rangle \\ |\Phi_4^3\rangle &= c_{1\uparrow}^\dagger c_{2\downarrow}^\dagger c_{4\downarrow}^\dagger |0\rangle & |\Phi_5^3\rangle &= c_{1\uparrow}^\dagger c_{2\downarrow}^\dagger c_{5\uparrow}^\dagger |0\rangle & |\Phi_6^3\rangle &= c_{1\uparrow}^\dagger c_{2\uparrow}^\dagger c_{5\downarrow}^\dagger |0\rangle \\ &etc. \end{aligned} \quad (4)$$

Next, with respect to this basis set we construct the Hamiltonian matrix of which elements are defined as

$$H_{kl}^3 = \langle \Phi_k^3 | H | \Phi_l^3 \rangle. \quad (5)$$

Note that the upper index “3” in Equations 4 and 5 means that the basis set and the Hamiltonian matrix elements are applied for the system with three electrons. This matrix is then diagonalized by using exact-diagonalization method [16] to obtain its energy eigenvalues and eigenkets, which we denote as E_n^3 and $|\Psi_n^3\rangle$, respectively. In addition, we also need to tabulate two other sets of basis kets, one corresponding to $N_e - 1 = 2$ electron system with $\frac{2N!}{(N_e-1)!(2N-N_e+1)!} = \frac{10!}{2!8!} = 45$ configurations, and the other one corresponding to $N_e + 1 = 4$ with $\frac{2N!}{(N_e+1)!(2N-N_e-1)!} = \frac{10!}{4!6!} = 210$ configurations. Having obtained all the energy eigenvalues and eigenkets for all systems with two electrons (E_n^2 and $|\Psi_n^2\rangle$), three electrons (E_n^3 and $|\Psi_n^3\rangle$), and four electrons (E_n^4 and $|\Psi_n^4\rangle$), respectively, we then construct the corresponding retarded Green function matrix of which elements can be computed through Lehmann representation for zero temperature as

$$G_{\alpha\beta}^R(\omega) = \frac{1}{Z} \sum_n \left[\frac{\langle \Psi_0^3 | c_\alpha | \Psi_n^4 \rangle \langle \Psi_n^4 | c_\beta^\dagger | \Psi_0^3 \rangle}{\omega - (E_n^4 - E_0^3) + i\eta} + \frac{\langle \Psi_0^3 | c_\beta^\dagger | \Psi_n^2 \rangle \langle \Psi_n^2 | c_\alpha | \Psi_0^3 \rangle}{\omega + (E_n^2 - E_0^3) + i\eta} \right]. \quad (6)$$

Indices α and β indicate the combined site-spin coordinates of the initial and the final state of the electron system, ω represents the electron quasi-particle energy, η is a small real number that we may adjust numerically as necessary, R stands for “retarded”, while Z acts as the normalization factor.

We use the retarded Green function matrix to compute the corresponding spectral function matrix

$$[A(\omega)] = -\frac{1}{\pi} \text{Im} [G^R(\omega)]. \quad (7)$$

Further, we can compute the real part of optical conductivity using the Kubo formula, which for zero temperature is given by

$$\text{Re } \sigma(\omega) = \frac{\pi e^2}{\hbar a} \int_{\mu-\omega}^{\mu} dv \text{Tr}[v][A(v)][v][A(v+\omega)], \quad (8)$$

Here, $[v]$ is the velocity matrix of which elements may be approximated as $v_{\alpha\beta} = \frac{-t_{\alpha\beta}}{\hbar} a$, where $-t_{\alpha\beta}$ represents the corresponding hopping parameter connecting single-particle state α and β . Meanwhile, to obtain its imaginary part, we use the Kramers-Kronig relation:

$$\text{Im } \sigma(\omega) = -\frac{2\omega}{\pi} P \int_0^\infty d\omega' \frac{\text{Re } \sigma(\omega')}{\omega'^2 - \omega^2}. \quad (9)$$

Our main goal is to explore the optical properties of our model. For this purpose, we need the complex dielectric function, which we can directly obtain from the complex optical conductivity through the relation of

$$\varepsilon(\omega) = \varepsilon(\infty) + \frac{i\sigma}{\varepsilon_0 \omega}, \quad (10)$$

wherein our calculations we set $\varepsilon(\infty) = 1$. The final step of our calculation is to obtain the loss function (LF)

$$\text{LF}(\omega) = -\text{Im} \frac{1}{\varepsilon} = \frac{\varepsilon_2(\omega)}{\varepsilon_1^2(\omega) + \varepsilon_2^2(\omega)}. \quad (11)$$

This quantity measures the energy absorbed by the system from an external electron sent to pass the system. This quantity can experimentally be obtained from Electron Energy Loss Spectroscopy (EELS). This quantity is very important especially when we aim to study plasmons.

4. Results and Discussion

For all our calculation, we set the nearest-neighbor hopping parameter $t = 1$ eV, and the broadening parameter $\eta = 0.1$ eV. As for U and V , we vary the values as we present our results below.

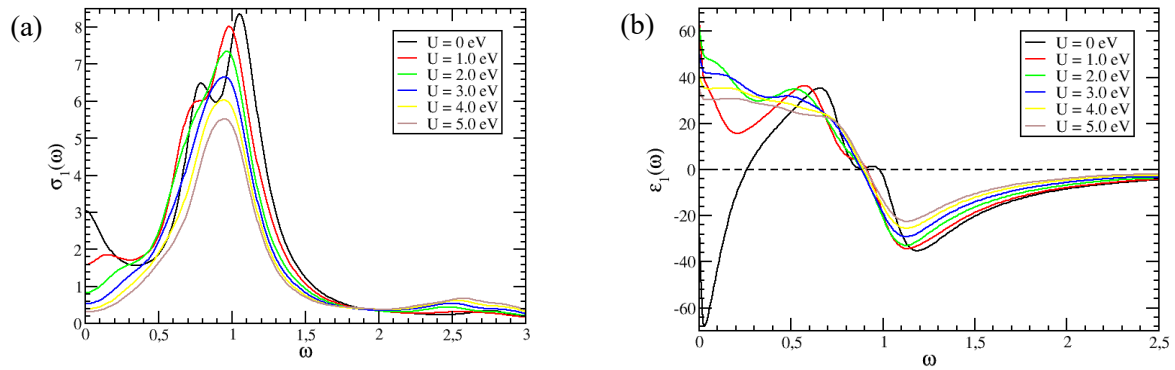


Figure 1. The real parts of optical conductivities and dielectric functions under variation of U with $V = 0$. (a) The real part of optical conductivities, and (b) real part of dielectric functions

Figure 1(a) shows the real part of optical conductivity ($\sigma_1(\omega)$) (in arbitrary unit) as a function of photon energy ω (in eV) for various U values, taking $V = 0$. Here we address several important points. The behavior of $\sigma_1(\omega)$ around $\omega = 0$ (the DC limit) as U is introduced and increased indicates a transition from metallic to insulating phase. When $U = 0$ the system clearly behaves as a metal characterized by the Drude peak around $\omega = 0$. As U is turned on, the DC conductivity ($\sigma_1(0)$) starts decreasing and vanishes as U becomes very large. The region around $\omega = 1$ eV and $\omega = 2.5$ eV where certain peaks exist indicate the existence of special electronic transitions or some quasi-particle excitations. We shall inspect these further through the real part of dielectric function.

Figure 1(b) displays the real part of the dielectric function ($\varepsilon_1(\omega)$) (in arbitrary unit) as a function of photon energy ω (in eV) also for various U values with $V = 0$. Close to the DC limit (ω around 0 – 0.5 eV), we see that $\varepsilon_1(\omega)$ evolves from being negative to positive values. This signifies the disappearance of a conventional plasmon at $\omega_p \approx 0.3$ eV, indicated by $\varepsilon_1(\omega_p) = 0$ when $U = 0$, as the system transforms from being a metal to an insulator. The structures around $\omega = 1$ eV around which $\varepsilon_1(\omega) = 0$ indicates the existence of other plasmons, which in some senses are similar to conventional plasmons because they are also indicated by $\varepsilon_1(\omega) = 0$, but they may not simply be considered as conventional plasmons by the fact that the crossings at zero of $\varepsilon_1(\omega)$ remain existing as the system has transformed into an insulator.

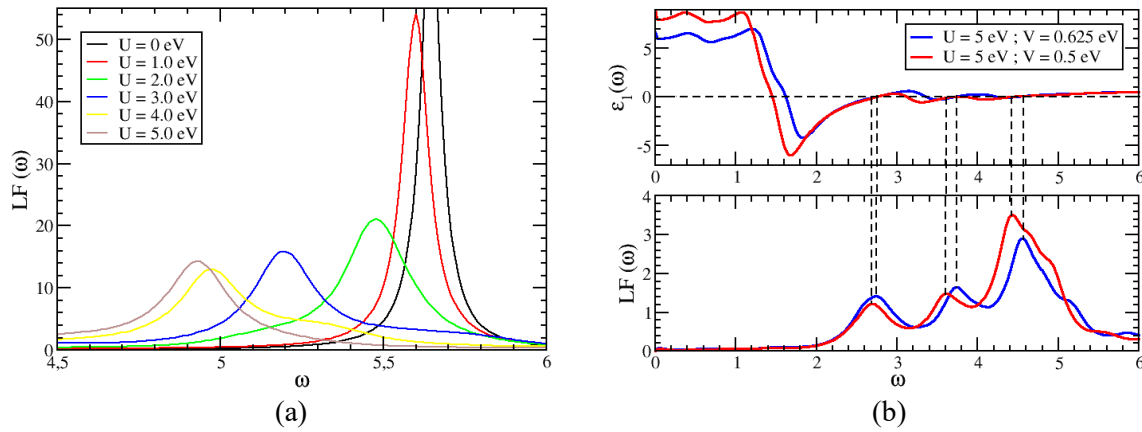


Figure 2. Loss functions (LFs) under variation of U . (a) Loss functions with $V=0$ and (b) with a variation of V compared to the dielectric functions.

Now we take a closer look at the plasmonic behavior for the system under variation of U with $V = 0$. Figure 2a shows the corresponding loss functions (LFs). It turns out that there are practically no significant peaks in the energy region below 4.5 eV (not shown), while the more pronounced plasmonic peaks appear around 5 eV as seen in Figure 3, which corresponds to another crossing at zero of $\varepsilon_1(\omega) = 0$ while the value of imaginary part of the dielectric function $\varepsilon_2(\omega)$ has become nearly vanishing (not shown). This observation suggests that the system initially has three plasmons, that is around 0.3 eV, 1 eV, and 5.6 eV. The one around 0.3 eV only exists in the metallic phase and vanishes as the system becomes insulating. The one around 1 eV remains, in principle, existing in both metallic and insulating phases. However, in spite of the fact that plasmons around 0.3 eV and 1 eV can theoretically exist, their physical existence may not be sensible by the experimental probe as their intensity is extremely weak compared to the third plasmon occurring around 5.6 eV. This 5.6 eV plasmon should be considered as unconventional as it has an unusually high plasmon frequency compared to typical ω_p values of common metals. Moreover, the plasmon frequency decreases (undergoes a red shift) as U increases but remains there as the system has become insulating. The nature of unconventionality of the plasmons arises to the combined effect of confinement (the reduction of the system size), and electron-electron interactions as indicated by the presence of U . Owing to this nature, we may suggest referring to this kind of plasmons as correlated plasmons.

Our main result is shown by the loss functions at $U = 5$ eV and $V = 0.5$ eV and 0.625 eV, which we compare with the corresponding real part of dielectric functions in Figure 2b. By including the inter-site Coulomb repulsion V with only relatively small values, i.e. $V = 0.1U = 0.5$ eV, and $V = 0.125U = 0.625$ eV, in the calculation, we see that there the additional plasmonic peaks arise in the loss function. Here, we intentionally adjust the U and V values so as to make our calculated loss function spectrum resembles that of the experimental data for the $\text{SrNbO}_{3.4}$ sample with extra oxygen planes in it [11]. The excellent qualitative similarity between the structure of three successive plasmonic peaks with ascending

intensity in our calculated loss functions and those observed in the experimental data of Ref. [11] is a signature that the hypothesis and model we present in this paper can be considered as a potentially legitimate explanation of the underlying mechanism of the appearance of the unconventional or correlated plasmons observed in $\text{SrNbO}_{3.4}$. At this point, despite the excellent similarity of our LF spectra to that of the experimental data of Ref. [11], however, we acknowledge that the structure of our calculated $\epsilon_1(\omega)$ at $U = 5$ eV and $V = 0.5$ eV and 0.625 eV has a dissimilarity in that our plasmonic frequencies still correspond to crossings at zero of the $\epsilon_1(\omega)$ curves, which is not the case in the experimental data in Ref. [11]. We take this issue as a subject of future development of our model.

5. Conclusion

We have presented a model and developed the method to generate unconventional plasmons in a correlated one-dimensional system represented by a reduced-size 1D modified Hubbard model. We interpret the results as the confinement (reduction of the system size to a nanometer scale) leads the system to have a new plasmonic character with a much higher plasmon frequency, which persists as the system has transform into insulation phase upon the increase of on-site Coulomb repulsion U . We refer to this kind of plasmons as correlated plasmons. Further, the incorporation of inter-site Coulomb repulsion V of a certain value leads our results to mimic the experimental loss function spectra of $\text{SrNbO}_{3+\delta}$, which strongly indicates that our model may be a potentially legitimate explanation of the underlying mechanism of the correlated plasmons in that system. We acknowledge that our model may be subject to further development as it still carries some dissimilarities in the results of the real part of dielectric function compared to that of the experimental data of $\text{SrNbO}_{3+\delta}$.

References

- [1] Dionne J A and Atwater H A 2012 Plasmonics: Metal-worthy methods and materials in nanophotonics *MRS Bulletin* **37** 717–24
- [2] Ritchie R H 1957 Plasma Losses by Fast Electrons in Thin Films *Physical Review* **106** 874–81
- [3] Bohm D 1951 D. Bohm and D. Pines, *Phys. Rev.* **82**, 625 (1951) *Phys. Rev.* **82** 625
- [4] Pines D 1956 Collective Energy Losses in Solids *Reviews of Modern Physics* **28** 184–98
- [5] Heber J 2009 Plasmonics: Surfing the wave *Nature* **461** 720–2
- [6] Lai Y P, Lin I T, Wu K H and Liu J M 2014 YP Lai, IT Lin, KH Wu, and JM Liu, *Nanomater. Nanotechnol.* **4**, 13 (2014). *Nanomater. Nanotechnol.* **4** 13
- [7] van Loon E G C P, Hafermann H, Lichtenstein A I, Rubtsov A N and Katsnelson M I 2014 Plasmons in Strongly Correlated Systems: Spectral Weight Transfer and Renormalized Dispersion *Physical Review Letters* **113**
- [8] Yin J, Krishnamoorthy H N, Adamo G, Dubrovkin A M, Chong Y, Zheludev N I and Soci C 2017 Plasmonics of topological insulators at optical frequencies *NPG Asia Materials* **9** e425
- [9] Stauber T, Gómez-Santos G and Brey L 2017 Plasmonics in Topological Insulators: Spin–Charge Separation, the Influence of the Inversion Layer, and Phonon–Plasmon Coupling *ACS Photonics* **4** 2978–88
- [10] Hsieh D, Xia Y, Qian D, Wray L, Dil J H, Meier F, Osterwalder J, Patthey L, Checkelsky J G, Ong N P, Fedorov A V, Lin H, Bansil A, Grauer D, Hor Y S, Cava R J and Hasan M Z 2009 A tunable topological insulator in the spin helical Dirac transport regime *Nature* **460** 1101–5
- [11] Asmara T C, Wan D, Zhao Y, Majidi M A, Nelson C T, Scott M C, Cai Y, Yan B, Schmidt D, Yang M, Zhu T, Trevisanutto P E, Motapothula M R, Feng Y P, Breese M B H, Sherburne M, Asta M, Minor A, Venkatesan T and Rusydi A 2017 Tunable and low-loss correlated plasmons in Mott-like insulating oxides *Nature Communications* **8** 15271
- [12] Eder R, van den Brink J and Sawatzky G A 1996 Intersite Coulomb interaction and Heisenberg exchange *Physical Review B* **54** R732–5
- [13] Calandra M, Merino J and McKenzie R H 2002 Metal-insulator transition and charge ordering in the extended Hubbard model at one-quarter filling *Physical Review B* **66** 195102
- [14] Hubbard J 1963 Electron Correlations in Narrow Energy Bands *Proceedings of the Royal Society*

- A: Mathematical, Physical and Engineering Sciences* **276** 238–57
- [15] Lieb E H and Wu F Y 1968 Absence of Mott Transition in an Exact Solution of the Short-Range, One-Band Model in One Dimension *Physical Review Letters* **20** 1445–8
- [16] Lieb E H and Wu F Y 2003 The one-dimensional Hubbard model: a reminiscence *Physica A: Statistical Mechanics and its Applications* **321** 1–27
- [17] Noce C and Cuoco M 1996 Exact-diagonalization method for correlated-electron models *Physical Review B* **54** 13047–51

Acknowledgements

The authors thank Universitas Indonesia for supporting this project through PITTA Research Grant No. 2285/UN2.R3.1/HKP.05.00/2018.